Plant Physiol. (1986) 82, 511–517
0032-0889/86/82/0511/07/$01.00/0

# Function of Rhizodermal Transfer Cells in the Fe Stress Response Mechanism of *Capsicum annuum* L.

Received for publication December 31, 1985 and in revised form May 25, 1986

ERNST-CHRISTIAN LANDSBERG
*Institut für Nutzpflanzenforschung, Pflanzenernährung, Technische Universität Berlin, Lentzeallee 55-57, 1000 Berlin 33, Federal Republic of Germany*

## ABSTRACT

**A variety of red pepper (*Capsicum annuum* L., cv Yaglik) responds to Fe deficiency stress with simultaneously enhanced $H^+$ extrusion, reduction of ferric ions and synthesis of malic and citric acid in a swollen subapical root zone densely covered with root hairs. It is demonstrated that these stress responses temporally coincide with the development of rhizodermal and hypodermal transfer cells in this root zone. During stress response the transfer cells show a marked autofluorescence which could arise from endogenous iron chelators of the phenolic acid type. The presence of organelle-rich cytoplasm which often exhibits rotational cytoplasmic streaming points to high physiological activity and makes these cells, with their increased plasmalemma surface, particularly well suited for the entire stress response mechanism. Since Fe stress-induced acidification is diminished by vanadate and erythrosin B, both specific inhibitors of plasmalemma ATPases, it seems reasonable to suppose that $H^+$ pumping from transfer cells is activated by an ATPase located in their plasmamembrane. $H^+$ extrusion is also shown to be inhibited by abscisic acid. Raised phosphoenolpyruvate carboxylase activity and simultaneous accumulation of malate in the swollen root zone point to the action of a pH stat preventing a detrimental rise in cytoplasmic pH of transfer cells during enhanced $H^+$ extrusion. The simultaneous increase in citric acid concentration favors chelation of iron at the site of its uptake and thus ensures long distance transport to the areas of metabolic demand. A direct link between citrate accumulation and ferric ion reduction as proposed in recent literature further supports the crucial role of transfer cells in the response to Fe deficiency stress.**

Rhizodermal transfer cells induced by mineral stress were first reported for the halophyte *Atriplex hastata* treated with high NaCl concentrations (13). The striking similarity of the accompanying morphological symptoms such as root tip swelling and root hair formation to analogous symptoms induced in Fe deficient sunflower plants (16) led to the discovery of transfer cells in Fe-starved roots (15). Even under salt stress conditions, the important role of iron nutritional status for the development of transfer cells is emphasized by the fact that their formation can be hindered by increasing Fe supply (14). This suggests that a NaCl-induced Fe shortage was the immediate trigger of transfer cell differentiation in that experiment.

In a first attempt to characterize the physiological function of transfer cells under Fe deficiency, it was proposed (18) that their development is related to enhanced $Fe^{III}$ reduction and $H^+$ efflux, both of which are well known key reactions of the so-called Fe stress response mechanism (for review see Ref. 5). On the other hand, Römheld and Kramer (27) stated in a comparative study of various plant species that transfer cell formation is directly related only to increased proton secretion. However, this generalization seems problematic. Their measurements of $Fe^{III}$ reduction were expressed for the fresh weight of excised roots in general and not for the actual transfer cell zone of only a few mm that varies substantially in length from species to species.

The purpose of the present paper is to provide a more detailed elucidation of the functional role of rhizodermal transfer cells under Fe deficiency stress. The results demonstrate that, at least for red pepper, these specialized cells are involved not only in proton secretion but are also related to enhanced $Fe^{III}$ reduction, organic acid accumulation and possibly the production of phenolic iron chelators.

## MATERIALS AND METHODS

**Growth of Plants.** Seeds of red pepper (*Capsicum annuum* L. cv Yaglik) were germinated and grown to the seedling stage in quartz sand moistened with $CaSO_4$ solution (0.2 mM). The seedlings were then transferred for 2 weeks to a continuously aerated nutrient solution that contained, in mM: $Ca(NO_3)_2$, 2.0; $K_2SO_4$, 0.75; $KH_2PO_4$, 0.50; $MgSO_4$, 0.65; $H_3BO_3$, $1.0 \times 10^{-2}$; $MnSO_4$, $1.0 \times 10^{-3}$; $CuSO_4$, $5.0 \times 10^{-4}$; $ZnSO_4$, $5.0 \times 10^{-4}$; $(NH_4)_6Mo_7O_{24}$, $5.0 \times 10^{-5}$; Fe as $Fe^{III}$EDTA, $2.5 \times 10^{-2}$.

All plants were grown in a controlled growth chamber with a day/night regime of 16/8 h and light intensity near 28 $W/m^2$ (fluorescent tubes, Osram-L 40 W/25 white and 40/77 Fluora, ratio 4:1). The temperature was 24°C (light and dark), the RH approximately 70%.

**pH Measurements.** To induce Fe deficiency plants were transferred to plastic jars (one plant per jar), containing 600 ml nutrient solution without FeEDTA. The pH of the solution was recorded continuously. After 3 to 4 d plants were selected which showed a similar degree of chlorosis and for which the pH decrease of the ambient medium started at nearly the same time.

Patterns of $H^+$ efflux from intact Fe-stressed roots were visualized as previously shown (18). Selected single roots were rinsed with distilled $H_2O$ and (remaining attached to the plant) placed into darkened Petri dishes filled with 0.6% agar medium containing Fe-free nutrient solution and bromocresol purple (50 mg $L^{-1}$) with a pH being adjusted to 5.8. The assembly was kept under the lights in the growth chamber.

For inhibitor studies orthovanadate solutions were prepared according to O'Neill and Spanswick (25). ABA stock solution was prepared by dissolving ABA in a minimal volume of KOH and neutralizing with HCl.

**Organic Acids.** Hot water extracts containing glutaric acid as internal standard were cleared by passage through cation and anion exchange resins (Dowex 50-X8, 200 to 400 mesh, $H^+$ form, and Dowex 1-X8, 200 to 400 mesh, formate form). After elution with 16 M HCOOH the anionic fraction was brought to dryness under vacuum at 40°C and taken up in 1-ml Reacti-

Vials for derivatization with MSTFA[1] which also served as solvent. After silylation at room temperature for 30 min 1-μl samples were analyzed by GC (Perkin Elmer F22 equipped with flame ionization detector) on a 2-m long glass column packed with 3% SE30. The temperature was 80 to 185°C at 5°C/min.

**PEP-Carboxylase Activity.** Samples (0.2–0.4 g fresh weight) from different root zones (swollen zone 0–8 mm, unswollen zone 10-20 mm behind tip) were ground with a cooled all-glass Potter-Elvehjem homogenizator in 6 volumes of extraction medium containing 50 mg insoluble PVP in 50 mM glycylglycine buffer, pH 7.4, with 10 mM 2-mercaptoethanol. After centrifugation at 80,000*g* for 20 min, crude extracts were desalted on Sephadex G-25 columns (Pharmacia, PD-10) and kept at 2°C until assayed the same day according to Smith and ap Rees (36). Enzyme activity per mg protein was calculated from the consumption of NADH during the reduction of oxaloacetate resulting from carboxylation of PEP. NADH was monitored with a Zeiss spectrophotometer (linear region of progress curves, 25°C). Soluble protein of the extracts was measured by a protein dye-binding method (4). Extraction and assay was carried out three times. Results never differed by more than 10%.

**Root Respiration.** $O_2$ uptake (μmol $O_2$/g fresh weight·h) of roots from individual intact plants was recorded with a Clark-type electrode (Orion Research) at different stages of Fe stress-induced acidification of the nutrient solution (kept at 25°C). During the measurement, the solution was layered with paraffin oil to restrict gas exchange with ambient air.

**Reducing Capacity.** Freshly cut root tips (5–8 mm length) from Fe-stressed plants were treated according to the slightly modified method of Olsen and Brown (23) using Ferrozine reagent, which forms a stable magenta complex species with $Fe^{II}$. The assay medium containing 0.2 mM Ferrozine, 0.5 mM $Fe^{III}$EDTA, 0.5 mM $CaSO_4$, and 10 mM sucrose was buffered with 5 mM Mes at pH 4.8. Sucrose was added in order to prevent a possible energy shortage due to root excision. During the experiment the solution (4 ml) was oxygenated by bubbling air and kept in the dark at 25°C for 60 to 120 min. The amount of $Fe^{II}$ resulting from the reduction of $Fe^{III}$ was determined by the absorbance of the $Fe^{II}$Ferrozine complex at 562 nm. The staining technique for the visualization of $Fe^{III}$ reduction along the root also involved complex formation of $Fe^{II}$ with Ferrozine.

In addition, *in situ* reducing capacity was localized according to Sijmons and Bienfait (33) using Nitro-BT, which is known to act as an electron acceptor in enzyme-catalyzed redox reactions whereby the colorless tetrazolium salts are converted to water- and lipid-insoluble dark blue colored formazans.

**Microscopy.** Cross-sections from fresh roots were obtained with a Leitz quick freezing microtome, mounted in 0.067 M phosphate buffer, pH 8.4, and immediately examined with a Zeiss photomicroscope. Fluorescence was tested using epifluorescence optics in conjunction with a beam splitter FT395, an exciter filter G365 and a barrier filter LP420 for UV-light excitation or the combination FT510, BP450-490 and LP520 for blue-light respectively. Illumination was provided by an HBO 200 mercury arc lamp. Photographs were taken on Ektachrome 400 daylight film rated at 1600 ASA.

EM was performed on specimens fixed in glutaraldehyde/$OsO_4$ and embedded in epoxy resin as described elsewhere (18). Ultrathin sections were examined in a Zeiss EM-9 electron microscope.

[1] Abbreviations: MSTFA, *N*-methyl-trimethylsilyltrifluoroacetamide; Ferrozine, disodium salt of 3-(2-pyridyl)-5,6-(4-phenylsulfonic acid)-1,2,4,-triazine; Nitro-BT, 2,2′-di-*p*-nitro-phenyl-5,5′-diphenyl-3,3′-(3,3′-dimethoxy-4,4′-biphenylene)ditetrazolium chloride; DES, diethylstilbestrol; DCCD, dicyclohexylcarbodiimide; TIBA, 2,3,5-triiodobenzoic acid; PEP, phosphoenolpyruvate.

## RESULTS

**Physiological Response to Fe Deficiency Stress.** Plants growing in FeEDTA-free nutrient solution turned moderately chlorotic (pale yellowing of the youngest leaves) after the 4th d of Fe deprivation. Shoot and root growth were not noticeably affected at that time. Simultaneously, the main root and many newly developed laterals showed a typical subapical swelling densely covered by root hairs (Fig. 2a) and displayed strong autofluorescence under UV- or blue-light (Figs. 2b and 3). Controls did not exhibit this response (Fig. 2b). Cross-sections demonstrate that the fluorescence predominantly comes from the rhizodermal cell layer (Fig. 4).

The pH of the nutrient solution rapidly decreased at this stage from about 6.8 to values below 4.0. Root respiration was slightly increased during peak proton extrusion (about 25% of the controls). Adding orthovanadate, a well known inhibitor of plasmamembrane ATPases (25), to the nutrient solution at the beginning of the pH drop slowed the rate of pH decrease almost immediately (Fig. 1A). The same effect (not shown in the graph) was achieved with erythrosin B (30 mM), another plasmalemma ATPase inhibitor (20), and with ABA (Fig. 1A). DES and DCCD, recently used as ATPase inhibitors with Fe-deficient sunflower roots (30) did not prove useful because even the low concentrations of ethanol needed for solubilization significantly interfered

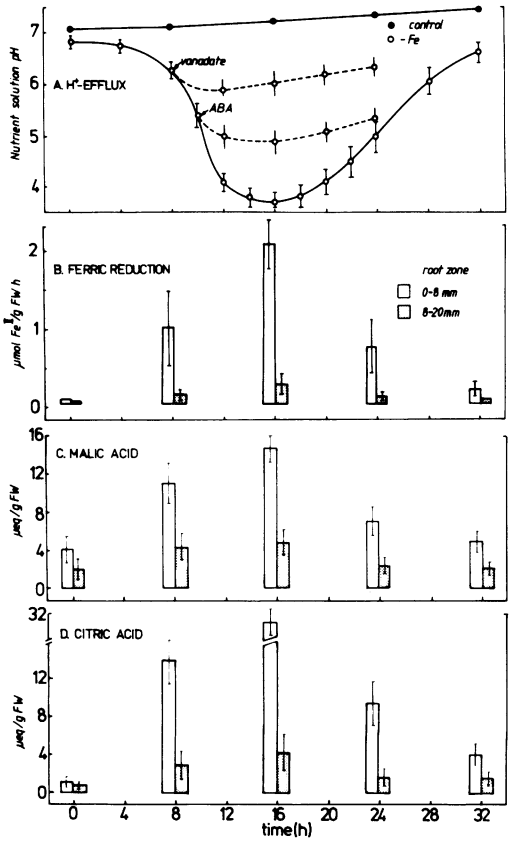


FIG. 1. Effect of Fe deficiency stress on simultaneous $H^+$-efflux, ferric reduction and organic acid content of red pepper roots. Fe-sufficient plants transferred to Fe-free solution started responding to Fe stress after about 4 d of Fe deprivation (time 'zero' on abscissa) by dropping the pH of the nutrient solution (A). Vanadate or ABA were added to the solution during pH decrease (arrows). At selected points of the pH drop swollen root tips (0–8 mm) and the proximal unswollen zone (8–20 mm) were excised and analyzed for their capacity to reduce ferric to ferrous iron measured as $Fe^{II}$Ferrozine (B) and for malic (C) and citric acid (D) accumulation. Experiments were the mean of four replications ± SE.

with $H^+$ efflux of red pepper.

Simultaneously with pH drop the reducing capacity of the swollen root zone increased as compared to the proximal unswollen zone (Fig. 1B). The slight rise shown for the latter may be attributed to the partial development of new short laterals in this area.

During the pH drop the concentration of malic and citric acid also rose markedly, primarily in the root swelling (Fig. 1, C and D), where the stress-induced proton efflux is located (Fig. 5). It was accompanied by a 185% increase of PEP-carboxylase activity in this zone, while in the proximal unswollen root area the enzyme activity remained nearly constant.

The short-term incubation in the agar medium made it possible to exactly distinguish between the subapical swelling zone and the apical meristem: increased $H^+$ efflux obviously is restricted to the former (Fig. 5). The enhanced $Fe^{III}$ reduction is also exactly confined to the root swelling (Fig. 6). Contrary to the results of Römheld and Marschner (28), who stated that iron reduction in roots of Fe-stressed plants also takes place at the apical meristem, Figure 6 clearly demonstrates the absence of enhanced reduction at the apex. This is corroborated by similar results obtained for Fe deficient bean roots (33).

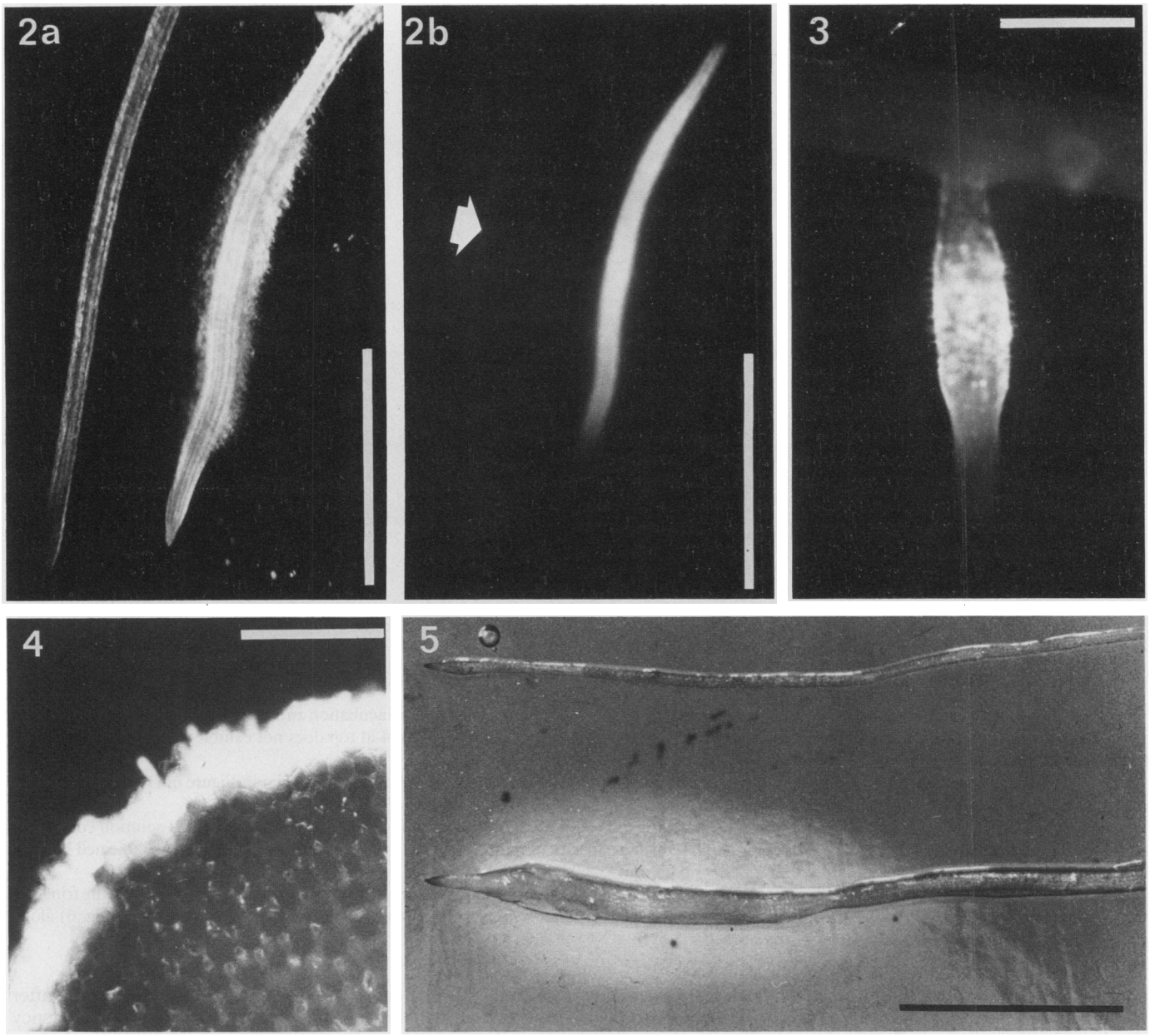


FIG. 2. Paired dark field (2a) and epifluorescence (2b) photographs of the same red pepper root tip during Fe stress response. Control root on left in each picture. Stress-induced autofluorescence is confined to the subapical swollen root zone densely covered with root hairs. Control (arrow) does not show autofluorescence. Marker bar = 5 mm.

FIG. 3. Fe stress-induced autofluorescence in the subapical swelling of a young lateral root. Marker bar = 1.5 mm.

FIG. 4. Cross section of stress-induced swollen root zone (3 mm behind tip) showing autofluorescence confined to the rhizodermal cell layer. Marker bar = 0.1 mm.

FIG. 5. Fe stress-induced $H^+$ efflux from subapical swollen root zone of an intact red pepper plant. Made visible through a 10 min incubation of the root in agar medium mixed with bromocresol purple (pH adjusted to 5.8). Acidification is shown by the light area (yellow in the original color print). Control root (at top) does not show any acidification. Marker bar = 5 mm.

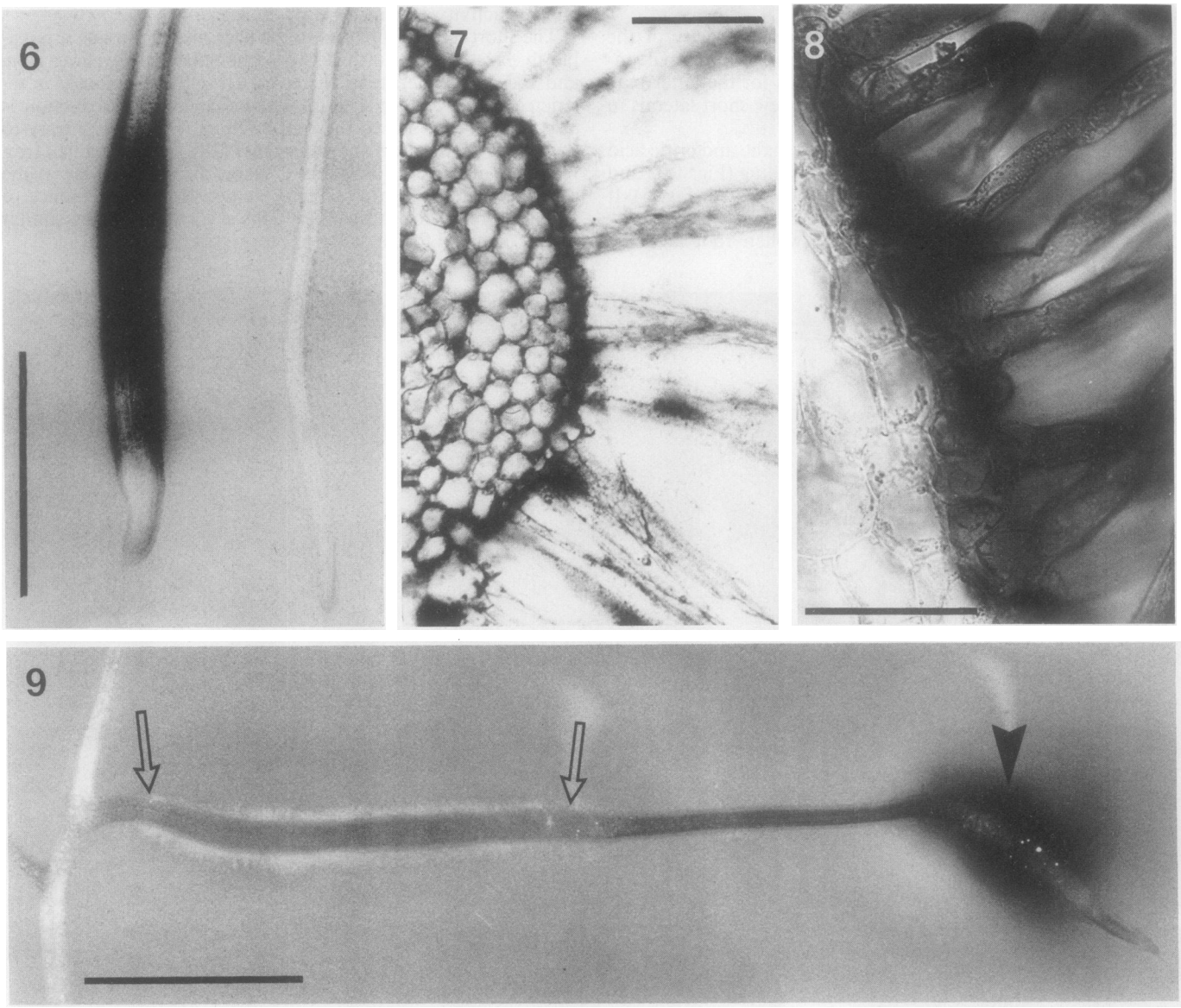


FIG. 6. Fe stress-induced ferric reduction along a subapical swollen root zone after a 10 min incubation in Ferrozine test solution. Dark area (purple-red coloration on the original color print) indicates formation of $Fe^{II}$Ferrozine. Control root at top does not exhibit visible ferric reduction. Marker bar = 5 mm.

FIG. 7. Ferric reduction site on freshly prepared cross section of a swollen root zone (3 mm behind tip) as shown in Figure 6. Dark areas indicate $Fe^{II}$Ferrozine formation in the rhizodermis after 10 min incubation in test solution. Marker bar = 0.1 mm.

FIG. 8. Cross section of a swollen root zone (3 mm behind tip) made 10 min after incubation in 0.1 strength Fe-free nutrient solution containing 100 $\mu$M tetrazolium salt Nitro-BT as electron acceptor. High reducing capacity of the rhizodermal cell layer including root hairs is indicated by dark blue coloration due to tetrazolium reduction. Marker bar = 0.05 mm.

FIG. 9. Locus of ferric reduction in response to alternating Fe deficiency stress. Area between arrows shows prior root swelling with fringe of short root hairs (first Fe stress response). Pointer indicates current site of ferric reduction (dark coloration due to $Fe^{II}$Ferrozine as in Fig. 6) along new swelling zone (second Fe stress response). Marker bar = 5 mm.

Freshly prepared transverse sections taken from the root swelling indicate that the reduction sites primarily are confined to the rhizodermal cell layer including root hairs (Fig. 7). A similar result was obtained using Nitro BT, which forms dark blue insoluble diformazan after reduction in the rhizodermis (Fig. 8).

The biochemical Fe stress response reactions clearly are of transient nature; within about 8 h after peak proton release and production of reductants and organic acids the values of each component started returning to their initial levels (Fig. 1), probably resulting from mobilization of iron precipitated as ferric hydroxide or ferric phosphate at the root surface and in the free space during preculture with FeEDTA. New apical growth with a 'normal' rate of elongation started immediately. However, after continued growth in the FeEDTA-free solution Fe deficiency occurred again and the described change in root tip morphology was repeated (Fig. 9). Furthermore, this picture demonstrates that $Fe^{III}$ reduction only occurs at the newly built root thickening.

**Cytological Response to Fe Deficiency Stress.** Electron microscopic investigation of Fe-stressed roots revealed the occurrence of numerous transfer cells in the rhizodermis and hypodermis of the swollen root zone. Serial sectioning confirmed that these cells do not occur in the meristematic zone of the root apex nor in the unswollen proximal root part. Figure 10 represents a typical rhizodermal transfer cell with dense cytoplasm and labyrinthian

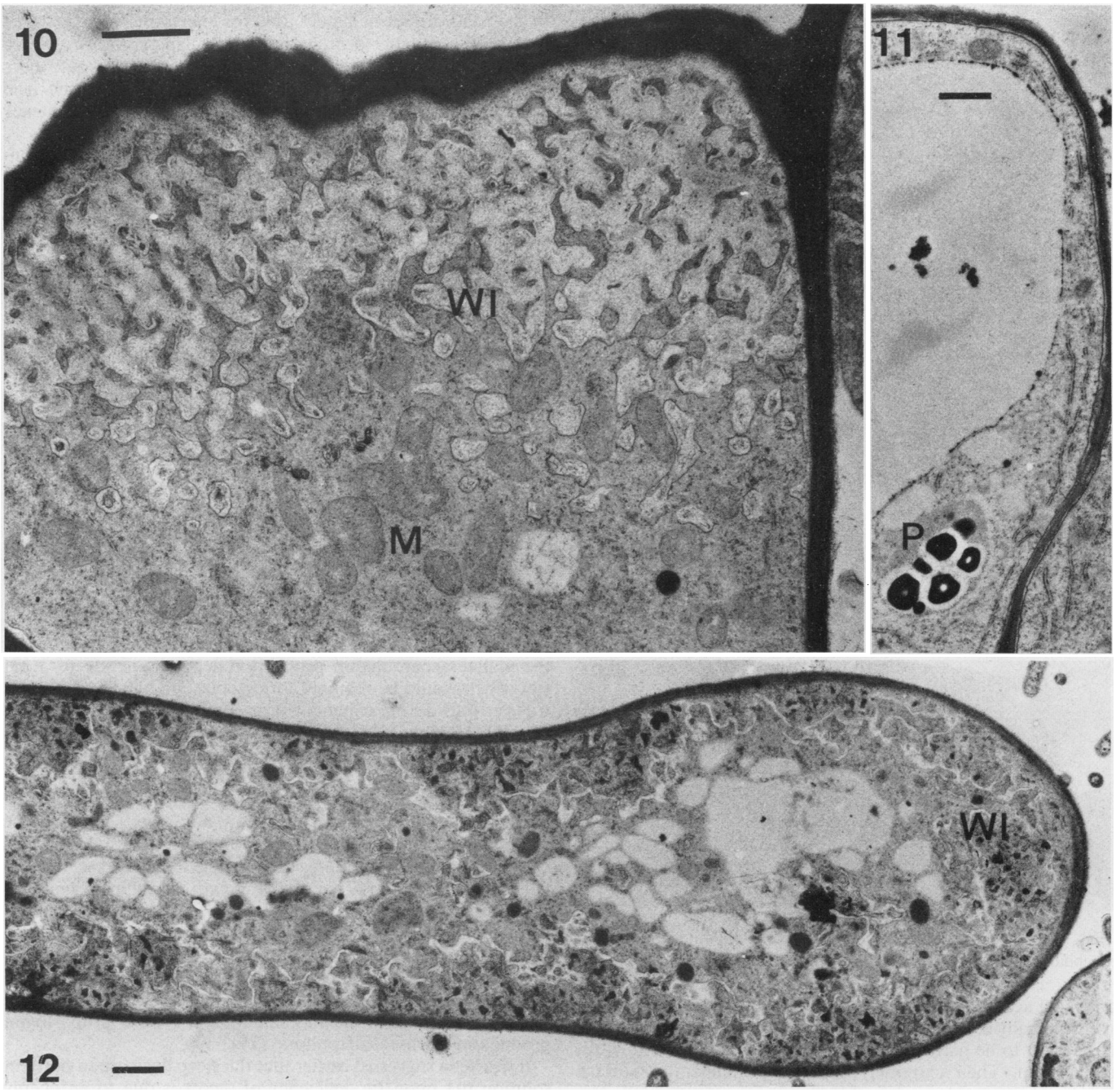


FIG. 10. Epidermal transfer cell with extremely elaborated wall ingrowths (WI) on the outer cell wall and accumulation of mitochondria (M) (×14,500). Marker bar = 1 μm.

FIG. 11. Epidermal cell of control root. Plastid (P) with starch grains (×8,400). Marker bar = 1 μm.

FIG. 12. Root hair with wall ingrowths and high proportion of cytoplasm (×6,000). Marker bar = 1 μm.

cell wall protuberances on the outer tangential walls. Rhizodermal cells of control roots are totally devoid of wall ingrowths and are highly vacuolated (Fig. 11). Young root hairs also show transfer cell features (Fig. 12). Under suitable dark field illumination, root hairs often displayed rotational cytoplasmic streaming along their longitudinal walls.

The characteristic enrichment in mitochondria and plastids of transfer cells is shown in more detail in Figure 13. The plastids are lacking fully developed starch grains even when samples were taken from plants which performed the stress response reactions at the end of the light period. Their often amoeboid shape with invaginations which sometimes encircle mitochondria probably favors intense metabolite exchange. The plastids of Fe sufficient rhizodermal cells are much less variable in shape and are densely packed with starch bodies (Fig. 11).

As soon as maximum activity of the Fe stress response reactions drops, the transfer cells start degenerating: the amount of cytoplasm decreases, a large central vacuole is formed and the cell wall protuberances redifferentiate to remnants of the former wall labyrinth.

## DISCUSSION

This paper demonstrates that transfer cell formation spatially and temporally coincides with the action of the three main Fe stress response reactions: proton efflux, $Fe^{III}$ reduction and or-

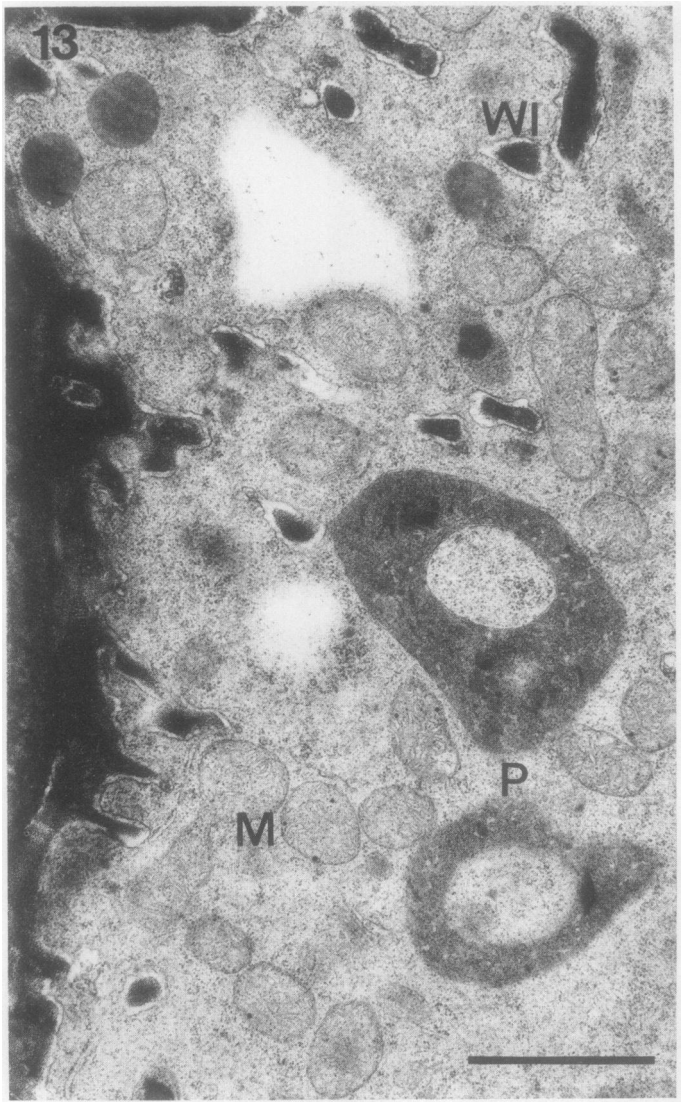


FIG. 13. Hypodermal transfer cell with numerous mitochondria and amoeboid plastids (P) (×18,500). Marker bar = 1 μm.

ganic acid accumulation. Since $Fe^{III}$ reduction has proven to be an enzymically controlled membrane-bound process (3), transfer cells appear to be particularly well suited for reduction of extracellular iron. Their extremely enlarged plasmalemma surface leads to an increased number of $Fe^{III}$ reducing sites per cell. The root surface enlargement already achieved by enhanced root hair formation in this zone (Fig. 2a) is thus additionally amplified. The labyrinthian cell wall system protruding far into the cytoplasm would shorten transport distances between the plasma membrane-localized redox system and the cytosolic compartments for delivery of reductant power. Bienfait *et al.* (3) showed that the apparent pH optimum of the $Fe^{III}$ reducing system is rather low. Increased trans-plasmalemma ferricyanide reduction has been shown in response to fusicoccin which is known to activate $H^+$ efflux (8). The location of both $Fe^{III}$ reduction and proton pumping sites in the plasmalemma of transfer cells would thus allow efficient coupling of the two processes. Additionally, the protonmotive force arising from high proton extrusion could be used for $Fe^{II}$ uptake directly at the reduction sites.

The almost complete disappearance of visible starch grains in transfer cell plastids, together with the increased number of mitochondria (Fig. 13), points to intense carbohydrate oxidation during stress response. Probably most of the sugars transported to the roots are immediately used for energy delivery or stored in an easily available form, so that no starch deposits are retained as in Fe sufficient roots. A high energy turnover would be a prerequisite not only for proton extrusion and organic acid accumulation but also for sufficient supply of NADPH, the key electron donor for $Fe^{III}$ reduction (33).

It was recently proposed that citrate accumulation may contribute via cytosolic isocitrate dehydrogenase activity to high NADPH levels and thus increase $Fe^{III}$ reduction (2). This corresponds with the accumulation of citric acid in the swollen root zone and the numerous mitochondria in transfer cells since citric acid synthesis takes place in these organelles. In addition, citrate is well known as a specific chelator for iron (37) and would thus ensure its long distance transport directly from the sites of reduction and uptake to the areas of metabolic demand. Citrate accumulation under Fe deficiency has been thought to be caused by a decrease in the activity of the iron-containing mitochondrial enzyme aconitase which mediates the conversion of citric acid to aconitic acid in the Krebs cycle (1). During acidification, however, no decrease in enzyme activity could be detected (EC Landsberg, unpublished data), suggesting that at this early stage of Fe deficiency the iron supply of the mitochondria is not yet markedly impaired. This may also be indicated by the slightly enhanced root respiration during stress response.

The marked rise in PEP-carboxylase activity and malate concentration during $H^+$ efflux indicate an elevated $CO_2$ dark fixation rate. This could serve to replenish the Krebs cycle for increased citrate export from the mitochondria during stress response and thus guarantee its continued operation. In addition, the malate accumulation probably reflects the action of a pH stat which would be required for cytoplasmic pH control in the transfer cells during enhanced proton extrusion. Such a mechanism has already been shown for other physiological processes where large pH changes have to be balanced by organic acid synthesis (35).

Organic acid accumulation was also reported for roots of Fe deficient grasses which did not show any acidification of the nutrient solution (17). However, a marked accumulation was only detectable after prolonged Fe deficiency when severe chlorosis had developed (17) and root growth as well as respiration were already significantly diminished (EC Landsberg, unpublished data). The organic acid buildup thus appears to be the result of a disturbed metabolism rather than part of a control mechanism. This fits into the model recently proposed for Fe stress response of grasses which does not depend on acidification and $Fe^{III}$ reduction at the plasmalemma but rather primarily on production of phytosiderophores (29).

It has been suggested earlier that the steep decrease in nutrient solution pH upon Fe deficiency of dicots is due to an energy driven $H^+$ efflux pump mediated by a plasmamembrane ATPase (17, 18). The inhibition of pH lowering after treatment with vanadate and erythrosin B, both specific inhibitors of plasmalemma ATPases (20, 25), supports this hypothesis. Fe stress-induced proton extrusion is thought to be the most active $H^+$ efflux pump so far known in roots of intact plants (30). It has to be distinguished from $H^+$ efflux coupled to transmembrane electron transport of the $Fe^{III}$ reducing system which takes place only in the presence of extracellular electron acceptors and does not reach such high rates of $H^+$ efflux (34).

Up to now it was not known what signals control $H^+$ pumping induced upon Fe stress. The transfer cells could perhaps function as target cells for a hormonal control of this pump. Auxin may be assumed to be involved here in a similar way as in the classical coleoptile system (7) or in acidification performed by pea root microsomal vesicles (11). The decreased rate of $H^+$ efflux upon treatment of Fe deficient plants with ABA (Fig. 1A) might indirectly argue for this assumption since ABA has been shown

to antagonize auxin-induced $H^+$ efflux in oat coleoptiles or rape protoplasts (26, 32). Furthermore, a decrease in Fe stress-induced $H^+$ efflux was observed upon treatment of Fe deficient plants with TIBA (17, 19), a presumed inhibitor of polar auxin transport which also prevents the development of auxin-mediated $H^+$ efflux during gravitropic curvature of roots and phototropic curvature of sporophytes (9, 22). It is tempting to speculate that the changes in organic acids which occur during Fe stress response could be subject to a similar hormonal control mechanism: auxin has been shown to stimulate malic acid synthesis during $H^+$ efflux from elongating oat coleoptile segments as well as citrate synthase purified from bean root tips (12, 31). More detailed research on a possible involvement of hormones in the regulation of Fe stress response including transfer cell differentiation seems highly desirable.

Another interesting feature of Fe stress-induced transfer cells of red pepper is their strong autofluorescence (Figs. 2–4). To date, one can only speculate on the chemical nature of these fluorescing substances: since siderophore compounds of phenolic acid type are known for their typical autofluorescence under UV light (10), similar iron chelating phenolics may be synthesized by transfer cells and, by analogy to soil fungi, excreted into the soil solution. Enhanced exudation of a light-blue fluorescing compound by roots of Fe efficient soybeans was reported earlier (6). A phenolic Fe ligand excreted by Fe-stressed tomato roots has been found by Olsen *et al.* (24). Binding to such endogenous chelators would prevent rapid precipitation of ferric ions in the rhizosphere and thus aid their transport at least through the free space of the labyrinthian cell wall system to the actual reduction and uptake sites at the plasmamembrane. Further studies are needed to identify the chemical structure of the fluorescent compounds and to investigate their role in the Fe stress response of transfer cells.

*Acknowledgments*—The author is indebted to Mrs. U. Ortmann and Mrs. C. Wolfram-Wienberg for excellent technical assistance.

## LITERATURE CITED


1. Bacon JSD, PC Dekock, J Palmer 1961 Aconitase levels in the leaves of iron-deficient mustard plants (*Sinapis alba*). Biochem J 80: 64–70
2. Bienfait HF, PC Sijmons 1984 Biochemical basis of Fe efficiency in dicotyledonous plants. *In* Proceedings of the VIth International Colloquium for the Optimization of Plant Nutrition, Montpellier, France, pp 15–16
3. Bienfait HF, RJ Bino, AM Van der Bliek, JF Duivenvoorden, JM Fountaine 1983 Characterization of ferric reducing activity in roots of Fe-deficient *Phaseolus vulgaris*. Physiol Plant 59: 196–202
4. Bradford MM 1976 A rapid and sensitive method for the quantitation of microgram quantities in protein utilizing the principle of protein-dye binding. Anal Biochem 72: 248–254
5. Brown JC 1978 Mechanism of iron uptake by plants. Plant Cell Environ 1: 249–257
6. Brown JC, RS Holmes, LO Tiffin 1961 Iron chlorosis in soybeans as related to the genotype of root stalk. 3. Chlorosis susceptibility and reductive capacity at the root. Soil Sci 91: 127–132
7. Cleland RE 1982 The mechanism of auxin-induced proton efflux. *In* PF Waring, ed, Plant Growth Substances 1982. Academic Press, New York, pp 23–31
8. Craig TA, FL Crane 1985 Redox potential of the donor and the $H^+$ release of the transplasmalemma redox system of carrot cells. Plant Physiol 77: S-145
9. Ellis JG IV, RJ Thomas 1985 Phototropism of *Pellia*: evidence for mediation by auxin-stimulated acid efflux. J Plant Physiol 121: 259–264
10. Fekete FA, JT Spence, T Emery 1983 A rapid and sensitive paper electrophoresis assay for the detection of microbial siderophores elicited in solid-plating culture. Anal Biochem 131: 516–519
11. Gabathuler R, RE Cleland 1985 Auxin regulation of a proton translocating ATPase in pea root plasma membrane vesicles. Plant Physiol 79: 1080–1085
12. Haschke HP, U Lüttge 1975 Stoichiometric correlation of malate accumulation with auxin-dependent $K^+$-$H^+$ exchange and growth in *Avena* coleoptile segments. Plant Physiol 56: 696–698
13. Kramer D 1978 Transfer cells in the epidermis of roots of the halophyte *Atriplex hastata* L. Naturwissenschaften 65: 339
14. Kramer D 1983 The possible role of transfer cells in the adaptation of plants to salinity. Physiol Plant 58: 549–555
15. Kramer D, V Römheld, EC Landsberg, H Marschner 1980 Induction of transfer-cell formation by iron deficiency in the root epidermis of *Helianthus annuus* L. Planta 147: 335–339
16. Landsberg EC 1979 Einfluß des Säurestoffwechsels und der Nitratreduktion auf Eisenmangel-bedingte Veränderungen des Substrat-pH-Wertes bei monokotylen und dikotylen Pflanzenarten. PhD thesis, Technical University of Berlin
17. Landsberg EC 1981 Organic acid synthesis and release of hydrogen ions in response to Fe deficiency stress of mono- and dicotyledonous plant species. J Plant Nutr 3: 579–591
18. Landsberg EC 1982 Transfer cell formation in the root epidermis: A prerequisite for Fe efficiency? J Plant Nutr 5: 415–432
19. Landsberg EC 1982 Shoot-root interactions in the regulation of Fe-deficiency stress-induced $H^+$ efflux from sunflower roots. *In* A Scaife, ed, Plant Nutrition 1982, Proceedings of the Ninth International Plant Nutrition Colloquium, Commonwealth Agricultural Bureaux, pp 310–315
20. Marre MT, G Romani, E Marrè 1983 Transmembrane hyperpolarisation and increase of $K^+$ uptake in maize roots treated with permeant weak acids. Plant Cell Environ 1: 249–257
21. Deleted in proof.
22. Mulkey JT, ML Evans 1982 Suppression of asymmetric acid efflux and gravitropism in maize roots treated with auxin transport inhibitors or sodium orthovanadate. J Plant Growth Regul 1: 259–265
23. Olsen RA, JC Brown 1980 Factors related to iron uptake by dicotyledonous and monocotyledonous plants. II. The reduction of $Fe^{3+}$ as influenced by roots and inhibitors. J Plant Nutr 2: 647–660
24. Olsen RA, JH Bennet, D Blume, JC Brown 1981 Chemical aspects of the Fe stress response mechanism in tomatoes. J Plant Nutr 3: 905–921
25. O'Neill SD, RM Spanswick 1984 Effects of vanadate on the plasma membrane ATPase of red beet and corn. Plant Physiol 75: 586–591
26. Rayle DL 1973 Auxin-induced hydrogen-ion secretion in *Avena* coleoptiles and its implications. Planta 114: 63–73
27. Römheld V, D Kramer 1983 Relationship between proton efflux and rhizodermal transfer cells induced by iron deficiency. Z Pflanzenphysiol 113: 73–83
28. Römheld V, H Marschner 1983 Mechanism of iron uptake by peanut plants. I. $Fe^{III}$ reduction, chelate splitting, and release of phenolics. Plant Physiol 71: 949–954
29. Römheld V, H Marschner 1986 Evidence for a specific uptake system for iron phytosiderophores in roots of grasses. Plant Physiol 80: 175–180
30. Römheld V, C Müller, H Marschner 1984 Localization and capacity of proton pumps in roots of intact sunflower plants. Plant Physiol 76: 603–606
31. Sarkissian IV 1972 Modification of enzyme activity, conformation and size by indoleacetic acid. *In* DJ Carr, ed, Plant Growth Substances 1970. Springer, Berlin, pp 265–271
32. Schubert S, H Matzke 1985 Influence of phytohormones and other effectors on proton extrusion by isolated protoplasts from rape leaves. Physiol Plant 64: 285–289
33. Sijmons PC, HF Bienfait 1983 Source of electrons for extra-cellular Fe(III) reduction in iron-deficient bean roots. Physiol Plant 59: 409–415
34. Sijmons PC, FC Lanfermeijer, AH de Boer, HBA Prins, HF Bienfait 1984 Depolarization of cell membrane potential during trans-plasma membrane electron transfer to extracellular elctron acceptors in iron-deficient roots of *Phaseolus vulgaris* L. Plant Physiol 76: 943–946
35. Smith FA, JA Raven 1979 Intracellular pH and its regulation. Annu Rev Plant Physiol 30: 289–311
36. Smith AM, T ap Rees 1979 Pathways of carbohydrate fermentation in the roots of marsh plants. Planta 146: 327–334
37. Tiffin LO 1966 Iron translocation. II. Citrate/iron ratios in plant stem exudates. Plant Physiol 41: 515–518